# Variations in the OM/OC ratio of urban organic aerosol next to a major roadway

Steven G. Brown [a] [b] , Taehyoung Lee [b] , Paul T. Roberts [a] & Jeffrey L. Collett Jr. [b]

[a] Sonoma Technology, Inc. , Petaluma , California , USA

[b] Atmospheric Science Department , Colorado State University , Fort Collins , Colorado , USA
Accepted author version posted online: 06 Aug 2013.Published online: 18 Nov 2013.

PLEASE SCROLL DOWN FOR ARTICLE

TECHNICAL PAPER

# Variations in the OM/OC ratio of urban organic aerosol next to a major roadway

Steven G. Brown,[1,2,*] Taehyoung Lee,[2] Paul T. Roberts,[1] and Jeffrey L. Collett, Jr.[2]

[1]*Sonoma Technology, Inc., Petaluma, California, USA*
[2]*Atmospheric Science Department, Colorado State University, Fort Collins, Colorado, USA*
*Please address correspondence to: Steven G. Brown, Sonoma Technology, Inc., 1455 N. McDowell Blvd., Petaluma, CA 94954, USA; e-mail: sbrown@sonomatech.com*

*Understanding the organic matter/organic carbon (OM/OC) ratio in ambient particulate matter (PM) is critical to achieve mass closure in routine PM measurements, to assess the sources of and the degree of chemical processing organic aerosol particles have undergone, and to relate ambient pollutant concentrations to health effects. Of particular interest is how the OM/OC ratio varies in the urban environment, where strong spatial and temporal gradients in source emissions are common. We provide results of near-roadway high-time-resolution $PM_1$ OM concentration and OM/OC ratio observations during January 2008 at Fyfe Elementary School in Las Vegas, NV, 18 m from the U.S. 95 freeway soundwall, measured with an Aerodyne high-resolution time-of-flight aerosol mass spectrometer (HR-AMS). The average OM/OC ratio was 1.54 ($\pm$ 0.20 standard deviation), typical of environments with a low amount of secondary aerosol formation. The 2-min average OM/OC ratios varied between 1.17 and 2.67, and daily average OM/OC ratios varied between 1.44 and 1.73. The ratios were highest during periods of low OM concentrations and generally low during periods of high OM concentrations. OM/OC ratios were low (1.52 $\pm$ 0.14, on average) during the morning rush hour (average OM = 2.4 $\mu g/m^3$), when vehicular emissions dominate this near-road measurement site. The ratios were slightly lower (1.46 $\pm$ 0.10) in the evening (average OM = 6.3 $\mu g/m^3$), when a combination of vehicular and fresh residential biomass burning emissions was typically present during times with temperature inversions. The hourly averaged OM/OC ratio peaked at 1.66 at midday. OM concentrations were similar, regardless of whether the monitoring site was downwind or upwind of the adjacent freeway throughout the day, though they were higher during stagnant conditions (wind speed < 0.5 m/sec). The OM/OC ratio generally varied more with time of day than with wind direction and speed.*

*Implications: Day-to-day variability in the fine particle OM/OC ratio is quite large, suggesting that using a fixed OM/OC value in PM mass closure calculations, even one that changes seasonally, may be insufficient to achieve accurate mass closure on individual days. Health studies that rely on OC measurements may under- or overestimate exposure to OM, and converting OC to OM with a fixed OM/OC ratio represents a significant source of uncertainty; thus, air quality managers may not have sufficient information about the importance of OM contributions to $PM_{2.5}$ to make optimal regulatory decisions.*

*Supplemental Materials:* Supplemental materials are available for this paper. Go to the publisher's online edition of the *Journal of the Air & Waste Management Association.*

## Introduction

Atmospheric particulate matter (PM) comprises a variety of materials, including crustal material; trace metals; ionic species such as sulfate, nitrate, and ammonium; and carbonaceous material. The carbonaceous fraction is composed of black or elemental carbon (BC, EC), which is emitted as a primary emission from combustion and is relatively unreactive in the atmosphere, and organic matter (OM). OM is made up of many different molecular structures and includes not only particulate organic carbon (OC), but also hydrogen, oxygen, nitrogen, and sulfur. Both PM, a large fraction of which can be OM, and specific molecules that are part of OM, such as polycyclic aromatic hydrocarbons (PAH), have been found to have health effects and to be carcinogenic (Larsen and Baker, 2003; Lobscheid and McKone, 2004; Adonis et al., 2003; Flowers et al., 2002). Together with BC, OM is the dominant component of the particulate fraction of vehicular exhaust (Schauer et al., 2002), which by itself has also been associated with health effects (Mauderly, 1994; Weingartner et al., 1997; Seagrave et al., 2006; Hiura et al., 2000). Effects evident in subjects living next to roadways include increased asthma rates, detrimental fetal development during pregnancy, decreased lung capacity, and increased cardiovascular disease (Health Effects Institute Panel on the Health Effects of

1422

Traffic-Related Air Pollution, 2010; Edwards et al., 1994; Nitta et al., 1993; Kim et al., 2004; Finkelstein et al., 2004; Kunzli et al., 2000; Hoek et al., 2002; Kan et al., 2010; 2008). Since OM is a substantial fraction of PM, characterizing the OM in particulate matter is important for understanding PM mass and its associated health effects.

While it is critical to understand OM concentrations, OM can be difficult to measure, especially on a routine basis. National-scale, routine $PM_{2.5}$ networks such as the Interagency Monitoring of Protected Visual Environments (IMPROVE) and Chemical Speciation Network (CSN) programs typically measure OC, but not OM. OM must be inferred from these OC measurements using an assumed OM/OC ratio. However, the OM/OC ratio can vary widely depending on source influences, monitoring location, season, and meteorology (Turpin and Lim, 2001; Bae et al., 2004; Aiken et al., 2008; Chan et al., 2010; Simon et al., 2011). Particulate matter containing more aliphatic hydrocarbons tends to have a lower OM/OC ratio (Russell, 2003; Turpin and Lim, 2001; Maria et al., 2003), while particulate matter dominated by secondary formation is typically more oxygenated and thus has a higher OM/OC ratio (Aiken et al., 2008). Even with high-resolution molecular speciation, typically only 10–30% of the OM can be quantified (Rogge et al., 1993; Volkamer et al., 2006), though improving techniques have been increasing the resolution of the unresolved complex mixture (Williams et al., 2010; Isaacman et al., 2012).

An accurate OM/OC ratio is necessary to achieve mass closure between gravimetric PM measurements and collocated measurements of PM constituents; to properly reflect the role of OM in regional and local air quality management plans; and to improve model predictions of OM (Polidori et al., 2008). The OM/OC ratio has also been used to characterize the relative level of oxidation of the organic material in the atmospheric aerosol as an estimate of the degree of chemical processing in the atmosphere (de Gouw et al., 2005, 2008; Aiken et al., 2009).

The OM/OC ratio in ambient air has been measured directly using high-resolution aerosol mass spectrometer (HR-AMS) measurements, as well as inferred via calculations using OC and other data. Chan et al. (2010) provided a review of key studies of OM/OC. For southern California, White and Roberts (1977) estimated an OM/OC ratio of 1.4, based on calculations of missing particulate mass that could not be explained by other measurements. This ratio of 1.4 has historically been used as a default value—for example, in the IMPROVE program (Malm et al., 1994). Turpin and Lim (2001) estimated OM/OC to be between 1.6 for urban organic aerosol and 2.1 for rural/aged organic aerosol, based on a survey of published speciated organic molecular marker data from multiple sites in the United States. Russell (2003) used Fourier transform infrared (FTIR) spectroscopy analysis of particulates on quartz fiber filters (QFF) and determined OM/OC to be, on average, 1.4, with a range of 1.2 to 1.6. Using 3 years of QFF analysis of organic molecular markers at an urban and rural site in the Midwest, Bae et al. (2006) estimated that OM/OC was between 1.5 and 1.9 at the rural site and between 1.3 and 1.6 at the urban site. Recently, Simon et al. (2011) developed a calculation of OM/OC by applying multilinear regression techniques and using many years of filter data collected from more than 100 sites in the United States, predominantly in rural areas, as part of the IMPROVE

program. They estimated OM/OC ratios to be, on average, between 1.37 and 1.94, with lower ratios in the western United States and during winter. Together, these studies provide a consistent range of estimates for OM/OC, though they are based on indirect measurements of OM and typically use 24-hr averaged samples.

With the development of the HR-AMS instrument (DeCarlo et al., 2006; Jayne et al., 2000; Jimenez et al., 2003) and associated data analysis techniques (Aiken et al., 2007), direct, high-time-resolution measurements of the elemental composition of nonrefractory $PM_1$ aerosol are possible. This means that the hydrogen-to-carbon (H/C), oxygen-to-carbon (O/C), and nitrogen-to-carbon (N/C) ratios of OM can be directly quantified, so a total OM concentration and an OM/OC ratio are obtained at high time resolution (e.g., at 2-min intervals). With these analysis techniques, Gilardoni et al. (2009) and Aiken et al. (2009) found that OM/OC ratios in the Mexico City area were between 1.6 and 1.8 in the urban area and between 1.8 and 2.1 aloft. In Riverside, CA (eastern Los Angeles area), during the winter, Williams et al. (2010) determined OM/OC to be, on average, 1.8. At a remote site in British Columbia, Sun et al. (2009) determined OM/OC to be 2.28 ($\pm$ 0.23). Chan et al. (2010) determined that OM/OC ratio values at a rural site in Ontario, Canada, were between 1.9 and 2.5.

OM/OC ratios have also been determined for a number of specific sources, and in particular for vehicular emissions. Using an HR-AMS, Chirico et al. (2010) found that the OM/OC ratio from vehicular emissions can vary between 1.26 at warm idle and 1.40 at cold idle, with other variations depending on the type of engine and operating condition. After 5 hrs of photochemical aging in a chamber, warm-idle and cold-idle OM/OC ratios increased to 1.45 and 1.63, respectively. Using a bottom-up approach in the development of a national-scale emissions inventory, Reff et al. (2009) estimated OM/OC ratios to be about 1.25 for vehicle exhaust. The OM/OC ratio of general laboratory-generated secondary organic aerosol (SOA) ranges from 1.4 to 2.7 (e.g., Kleindienst et al., 2007).

OM/OC is directly related to the H/C and O/C ratios of organic aerosol; higher O/C translates to higher OM/OC (Aiken et al., 2008). The ambient OM/OC depends not only on the emission ratio of OM sources and subsequent aging, but also on the volatility of the OM and how it partitions between the gas and particle phases (Kroll et al., 2011; Donahue et al., 2012). Higher OM concentrations lead to increased SOA yields from gaseous precursors (Donahue et al., 2012). Sage et al. (2008) noted that under high OM conditions, semivolatile and relatively unoxidized species can quickly contribute to OM concentrations via partitioning from the gas phase. The semivolatile material can also move into the particle phase via oxidation, leading to lower vapor pressures and subsequent partitioning; decreases in temperature and higher OM concentrations can also lead to increased gas-to-particle conversion of less oxidized species (Cappa and Jimenez, 2010).

Many of the ambient experiments described in the literature occurred at locations where a significant portion of the organic aerosol is transported some distance from emissions sources to the monitoring location, resulting in more aged, more oxidized organic aerosol and a higher observed OM/OC. Work has also been done in chemical aging chambers to assess the initial OM/

OC ratio of vehicular and other emissions and the process by which they may change over time in a controlled environment (Kroll et al., 2009; Mohr et al., 2009; Chhabra, et al., 2010; Tkacik et al., 2012), but little work has been done to characterize the OM/OC ratio of vehicular emissions in the near-roadway environment. In the short time from the emission of organic aerosol and semivolatile vapors from the tailpipe to their impact at a nearby receptor, nucleation, dilution, condensation, evaporation, and oxidation all affect the gas/aerosol organic mixture and its phase partitioning. With the HR-AMS, we directly determined OM/OC ratios in the near-roadway environment at Las Vegas, NV, based on measured H/C, O/C, and nitrogen-to-carbon (N/C) ratios of the ambient organic aerosol, which can be used to support photochemical modeling, to aid mass closure of PM, and to inform health studies. The OM/OC ratio is examined with respect to source influence and time of day.

## Methods

### Monitoring site location

Measurements were made next to a classroom and playground in Las Vegas, NV, at Fyfe Elementary School, directly adjacent to and 18 m from the U.S. 95 highway soundwall (see Figure 1 for a map, originally published in Brown et al., 2012). The focus of this paper is on intensive measurements taken during January 5–28, 2008, when OM/OC measurements were available; other air quality measurements occurred throughout 2007–2008. The U.S. 95 freeway has six lanes in each direction, with an annual average daily traffic (AADT) volume of 203,000 vehicles a day. A $3 \times 5$-m insulated shelter housed the meteorological, black carbon, and OCEC instruments, as described later. HR-AMS and particle-into-liquid-sampler (PILS) measurements were made in the Colorado State University (CSU) Mobile Laboratory, which was parked next to the main monitoring shelter during the study.



**Figure 1.** Location of monitoring equipment at Fyfe Elementary School.

The monitoring site is on the north side of the freeway, so the site is directly downwind of the freeway when winds blow from the south. North of the site is a residential area; the homes in the immediate neighborhood were built starting in the 1960s, and many have wood-burning fireplaces. Las Vegas is in a shallow bowl area, with mountains to the west and north, and is a relatively isolated, large urban area with a 2010 population of over 1.9 million in the greater metropolitan area of Clark County (http://quickfacts.census.gov/qfd/states/32/32003.html). There is little heavy industry in Las Vegas, with most $PM_{2.5}$ emissions coming from dust (e.g., http://www.epa.gov/air/emissions/pm.htm#pmloc); mobile sources comprise 9% of the emissions, but they account for 36% of the emissions if dust is excluded. A major electricity generation source listed in the most recent (2005) national emissions inventory (NEI) has since closed.

### HR-AMS description and data processing

The operation of the Aerodyne HR-AMS has been described in detail elsewhere (DeCarlo et al., 2006; Allan et al., 2004; Drewnick et al., 2005; Jimenez et al., 2003) and is only summarized here. Ambient air is drawn through a $PM_{2.5}$ cyclone and is sampled through a critical orifice into an aerodynamic lens, creating a narrow particle beam with a 50% passing efficiency of 1-μm particles so that essentially $PM_1$ is measured (Sun et al., 2009; Canagaratna et al., 2007). Particles with an aerodynamic diameter of 50 nm to 700 nm are collected with nearly 100% efficiency (Liu et al., 2007; Jayne et al., 2000); however, the HR-AMS may not fully quantify total particle mass if there is significant mass outside of this range. The sampling line is approximately 7 feet of ¼-inch diameter stainless steel tubing, with a bypass flow of 3 liters per minute (lpm) through the $PM_{2.5}$ cyclone and 0.1 lpm into the HR-AMS, resulting in an approximate residence time of 1.3 sec in the sampling line. The particles are accelerated in the supersonic expansion of gas molecules into a vacuum at the end of the lens. Particles are collected by inertial impaction onto a heated surface (600°C), and nonrefractory species such as nitrate, sulfate, ammonium, and OM are thermally vaporized. Vaporized gases undergo electron impact ionization and the charged fragments enter a time-of-flight mass spectrometer (ToF-MS) region, where they are separated by mass-to-charge ratio (*m/z*). After correction for interferences from ambient gases such as $N_2$ and $O_2$, mass spectra are analyzed for each 2-min averaged sample.

AMS measurements may not always have a collection efficiency (CE) of 100%, particularly in environments with a high fraction of mass from sulfate aerosol. However, in this study, as reported in Brown et al. (2012), the median sulfate concentrations were extremely low (median of 0.16 μg/m³); particulate matter with extremely low sulfate fraction can be collected with a CE of 1 by the HR-AMS (Matthew et al., 2008), which was used in this study. If the CE varied significantly by day or hour during the study, then we might be undermeasuring the OM, though it is unclear whether OM/OC would be biased low or high in that case. Results comparing AMS data with Sunset OC data, described later, indicate that a CE of 1 appears reasonable; as reported in Brown et al. (2012), HR-AMS and PILS $PM_{2.5}$ nitrate also compared well, assuming a CE of 1 ($r^2 = 0.95$,

median PILS/AMS ratio = 1.3), though with a positive bias toward the PILS measurements. The AMS was calibrated for nitrate ionization efficiency (IE) every week through introduction of 350-nm ammonium nitrate particles. Relative ionization efficiencies for other aerosol types were taken from published values (Aiken et al., 2008; DeCarlo et al., 2006).

AMS data were processed and analyzed using the standard AMS analysis software, Squirrel version 1.51, implemented with Wavemetric's Igor Pro (version 6.20). High-resolution (HR) data were processed with the AMS analysis software Pika version 1.10. The "W" path mode and calibration factors per Aiken et al. (2008) were used to analyze spectra for their elemental composition and to acquire H/C, O/C, and N/C, and therefore OM/OC, ratios of the organic aerosol signal. The OM/OC ratio is calculated from the organic aerosol signal in AMS mass spectra as shown in eq 1:

$$\frac{\left[12 + 1 * \left(\frac{H}{C}\right) + 16 * \left(\frac{O}{C}\right) + 14 * \left(\frac{N}{C}\right)\right]}{12}. \quad (1)$$

The OM/OC ratio is largely driven by the extent of oxidation in the organic aerosol; that is, the more oxygens associated with carbon in the aerosol, the higher the OM/OC ratio. For example, the PAH pyrene ($C_{16}H_{10}$) has a very low OM/OC of 1.05, and the long-chain alkane triacontane ($C_{30}H_{62}$) has an OM/OC ratio of 1.17. More oxidized species have higher OM/OC ratios. An example carboxylic acid, azelaic acid ($(CH_2)_7(CO_2H)_2$), has a ratio of 1.75, and levoglucosan ($C_6H_{10}O_5$), an anhydrous sugar with several OH groups, has an OM/OC of 2.25. With laboratory standards, Aiken et al. (2008) reported an average error of 6% when determining OM/OC values. AMS-inferred OC concentrations were also determined using the OM/OC ratio for each 2-min OM measurement, equal to the OM concentration divided by the OM/OC ratio. There were no extended (i.e., more than an hour) periods of downtime, except for daily calibrations.

## Sunset OCEC measurements

A Sunset OCEC instrument (Bae et al., 2004; Jeong et al., 2004; Bauer et al., 2009; Rattigan et al., 2010) measured organic and elemental carbon on an hourly basis. The Sunset OCEC instrument uses a thermal optical method similar to NIOSH 5040 (Chow et al., 2001; Sin et al., 2004) and has a limit of detection of 0.3 μg/m³ for OC and 0.01 μg/m³ for EC (Bauer et al., 2009). Particulate matter is drawn through a $PM_{2.5}$ cyclone inlet with a carbon denuder and deposited on a quartz fiber filter for 47 min. Particulate matter is then analyzed during an 8-min cycle by heating the filter to 840°C for 5 min to quantify OC, and then by introducing an oxidizing carrier gas (He with 10% $O_2$) at 850°C for 3 min to quantify EC. The remaining 5 min is used for cooling down the oven. During the filter heating, carbonaceous material evolves off the filter as $CO_2$, which is quantified via transmittance using a nondispersive infrared (NDIR) detector. EC is determined as any carbon evolved off the filter after the introduction of $He/O_2$ once the laser-monitored filter absorbance matches the initial absorbance measured when the filter was first heated. After each hourly analytical cycle, calibration gas of 5% $CH_4$ with He flushes the system. Instrument response is calibrated using a 99.9% reagent grade sucrose solution and a 5% $CH_4$/He calibration standard.

## Other collocated measurements

Meteorological data (wind speed, wind direction, temperature) were collected at 10 m above ground level (agl). Hourly meteorological data were vector-averaged. Each hourly observation was classified as downwind (wind speed greater than 0.5 m/sec and wind direction between 100 and 270 degrees); upwind (wind speed greater than 0.5 m/sec and wind direction between 310 and 60 degrees); other (wind speed greater than 0.5 m/sec and wind direction between 60 and 100 degrees or between 270 and 310 degrees); or stagnant (wind speed less than 0.5 m/sec). In addition, temperature was measured at 2 m agl. The difference between the 10-m and 2-m temperatures, which can be indicative of thermal inversions close to the ground, was used as an indicator of atmospheric stability; that is, the atmosphere was more stable when the 10-m temperature was higher than the 2-m temperature, as occurred on most evenings. In the daytime, the 2-m temperature was typically higher than the 10-m temperature.

Black carbon (BC) data at 880 nm wavelength were collected using a Magee Scientific Aethalometer, model AE-22, with a $PM_{2.5}$ inlet. One-minute data were processed into 5-min averages; time-stamp and filter tape spot saturation corrections were done using the Washington University Air Quality Lab AethDataMasher Version 6.0e (Washington University Air Quality Laboratory, 2006). CO data were collected using a Thermo Scientific 48i analyzer, yielding 1-min data with a manufacturer-specified lower quantifiable limit of 0.04 ppb and precision of 2%. The 1-min data were aggregated into 5-min data for validation. For hourly averages, 75% completeness of the 5-min averages was required. Automatic zero and span checks were performed each day for CO at 3:00 a.m., with a span value of 8 ppm. Both BC and CO can be used as indicators of vehicle emissions, though BC can also have some influence from residential biomass burning in the evening.

Traffic data were collected at the Torrey Pines overcrossing of U.S. 95, about 3.5 km from Fyfe Elementary, using a Wavetronix SmartSensor HD model 125. Hourly traffic speed plus volume by three size bins were measured: (1) small, vehicles with a length of 6 m (20 feet) or less; (2) medium, 6–12 m (21–40 feet) in length; and (3) large, longer than 12 m (40 feet).

# Results

## Overview of meteorological and traffic conditions and OM concentrations during study

Hourly averaged temperature varied between –1.6° and 15.5°C during the study. A summary of the wind speed and direction distribution is shown in Figure 2 as the fraction of observations that were classified as upwind, downwind, other, or stagnant, by hour of the day; a wind rose is provided in Brown et al. (2012). A typical diurnal pattern consisted of stagnant or upwind conditions at the site during evening, overnight, and early morning, followed by increased wind speeds from the south (i.e., downwind from the freeway) during late morning.
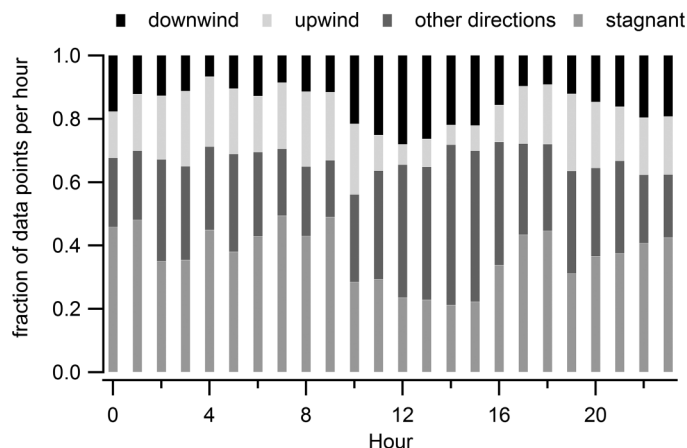
**Figure 2.** Fraction of 2-min AMS data points per hour by wind condition (downwind of freeway, upwind of freeway, parallel to freeway [other directions], or stagnant [wind speed less than 1 m/sec]).

Downwind conditions occurred most frequently in midday with sustained winds, while upwind conditions were typical in the evening. As indicated by the difference between the 10-m and 2-m temperatures, the atmosphere was typically stable overnight between 1700 and 0600 local standard time (LST).

Traffic was predominantly small vehicles, less than 21 feet in length, with an average weekday volume total of 167,000 vehicles/day, of which 90% were small vehicles. One percent of the total was large vehicles, those greater than 40 feet in length, with the remaining fraction made up of medium vehicles. The exact split between light-duty and heavy-duty vehicles is unknown. Conservatively, if half the medium vehicles and all of the large vehicles were heavy-duty diesel, then about 5% of the total would be heavy-duty diesel. Small vehicle volume peaked in the morning and evening, while large vehicle volume peaked in the late morning after the morning commute (i.e., 0900–1100 LST).

As discussed in Brown et al. (2012), OM averaged 3.3 μg/m$^3$ during the January study and was typically highest during the evening hours (i.e., 1900 through 2100 LST), with a secondary peak during the morning rush hour (i.e., 0600–0900 LST). Sulfate concentrations were extremely low throughout the study, with a median concentration of 0.16 μg/m$^3$ and a maximum 20-min average of 0.88 μg/m$^3$. These sulfate levels are quite low compared to most other areas in the United States but are not atypical in the western United States, as there is minimal transport of sulfate into Las Vegas and there are no major sources of SO$_2$ or sulfate upwind of the urban area. Nitrate concentrations were episodic but were also typically low, with a median concentration of 0.54 μg/m$^3$ and average of 1.09 μg/m$^3$.

Analysis of 2-min HR-AMS data with the U.S. Environmental Protection Agency (EPA) positive matrix factorization model, EPA PMF, yielded four factors that best accounted for the OM (Brown et al., 2012). On average, primary, hydrocarbon-like organic aerosol (HOA) made up 26% of the OM, while low-volatility oxygenated OA (LV-OOA) was highest in the afternoon and accounted for 26% of the OM. Biomass burning organic aerosol (BBOA) was evident only in the evening hours, came predominantly from the

residential area to the north, and, on average, constituted 12% of the OM; semivolatile OOA (SV-OOA) accounted for the remaining third of the OM, and was also highest in the evening hours. In areas with more aged aerosol, LV-OOA is relatively high, while HOA is more indicative of fresh emissions (Canagaratna et al., 2007; Docherty et al., 2008; Jimenez et al., 2009). HOA had a diurnal pattern that was similar to BC, with peaks in the morning and evening, while LV-OOA was highest at midday. In the evening, HOA combined with peaks of SV-OOA and BBOA, resulting in OM concentrations that were higher than in the morning. The varying OM mixture has an influence on OM/OC, as discussed later. Additional details and discussion of PMF results are provided elsewhere (Brown et al., 2012).

## Comparison between AMS and Sunset data

AMS-derived OC data were averaged for comparison to the hourly Sunset OC data. AMS PM$_1$ OC concentrations and Sunset PM$_{2.5}$ OC concentrations compared well (median difference = 0.05 μg/m$^3$, $r^2$ = 0.89, slope = 0.91; assuming $y$-intercept = 0) across all times of day, with the poorest relationship occurring when OC concentrations were less than 0.5 μg/m$^3$ (Figure 3). The average and median hourly OC$_{ams}$ concentrations during the study were 2.3 and 1.5 μg/m$^3$, while the average and median Sunset OC concentrations were 2.4 and 1.5 μg/m$^3$. The high correlation between the AMS and Sunset measurements is similar to results in Tokyo (Takegawa et al., 2005) and Pittsburgh (Zhang et al., 2005), where $r^2$ values were reported of 0.67–0.83 in two seasons and 0.88 in September, respectively. The correlation is much higher than the correlation reported in summer at Riverside (Docherty et al., 2011), where $r^2$ values were between 0.36 and 0.53 and where multiple Sunset instruments and methods were used; at Riverside the overall discrepancy between HR-
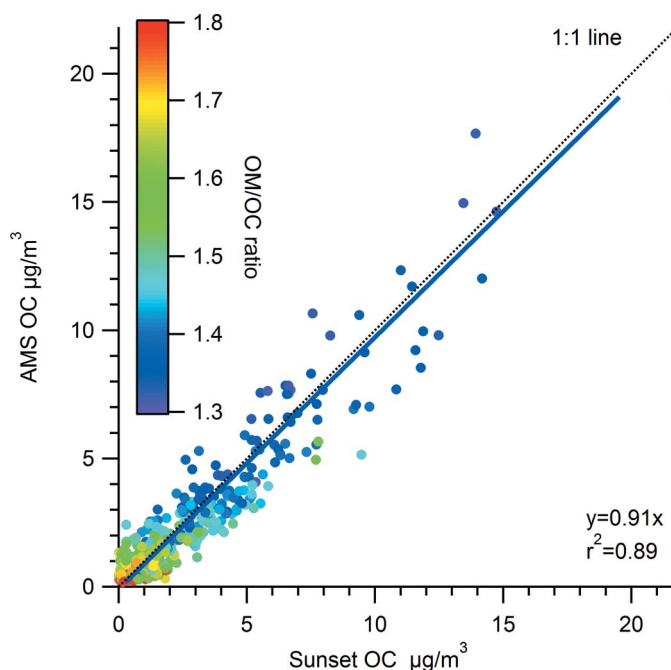


**Figure 3.** Hourly averaged AMS PM$_1$ OC and Sunset PM$_{2.5}$ OC concentrations (μg/m$^3$), colored by AMS-derived OM/OC ratio.

AMS and Sunset measurements was approximately 10%. In Las Vegas, the average $OM_{AMS}/OC_{Sunset}$ ratio was 1.56 ($\pm$ 0.08 95th percent confidence interval). This ratio is very similar to the average AMS-derived OM/OC ratio of 1.54 $\pm$0.01, though the $OM_{AMS}/OC_{Sunset}$ ratio was more variable.

## Daily patterns

Daily averaged HR-AMS OM/OC ratios varied between 1.44 and 1.73, with an average of 1.54, while daily concentration averages of OM were between 1.1 and 6.6 $\mu g/m^3$ (Figure 4). Generally the OM/OC ratio was low when OM was high; this occurred when stagnant conditions led to a buildup of OM concentrations (Figure 5). The lower OM/OC ratios are consistent with more fresh, primary aerosol, while the higher values mean more oxygen, hydrogen, and/or nitrogen associated with the organic aerosol, likely from atmospheric processing. Higher OM concentrations are also expected to cause increased partitioning of the semivolatile, less oxidized material to the particulate phase (Sage et al., 2008; Robinson et al., 2007), leading to lower OM/OC ratios. No clear relationship of OM/OC with temperature was evident in the data set (Supplemental Figure 1 and Brown et al., 2012), even though temperature plays a role in gas/particle partitioning and can, therefore, influence the ambient OM concentration. On a daily average basis, higher wind speeds were associated with higher OM/OC ratios. When the urban area is well ventilated we expect more oxidized, aged, regional aerosol to comprise a greater proportion of the OM, since fresh aerosol emissions are diluted and are more likely to partition into the gas phase than aged aerosol are. This relationship is clearer when examining hourly averages (discussed later). For the observed daily average OM/OC ratio range of 1.44 to 1.73, if OC is measured and OM calculated with the traditionally assumed urban OM/OC ratio of 1.4, then the estimate of OM for the Las Vegas period and location described here would be biased low by an average of 9% and as much as 17%. With more oxidized and secondary organic aerosol present during
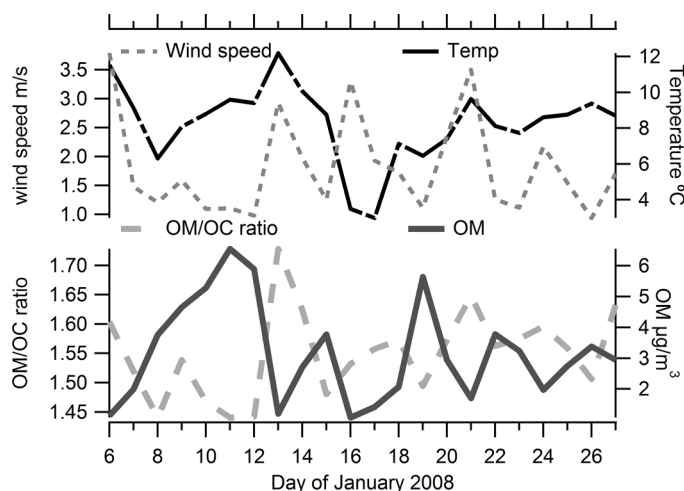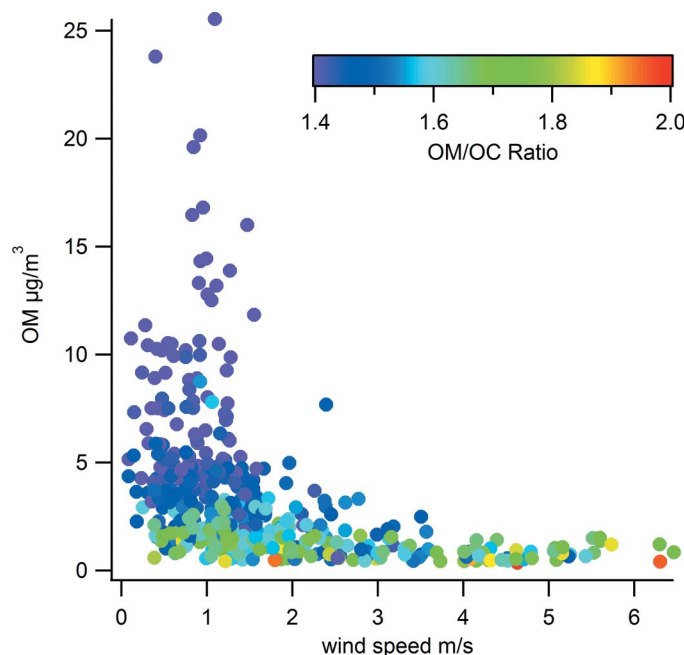


**Figure 5.** Hourly-averaged OM concentrations ($\mu g/m^3$) as a function of wind speed, colored by OM/OC ratio.

summertime, we anticipate the actual OM/OC value would be higher than observed in this winter study.

## Diurnal variations

Figure 6 summarizes the average diurnal variability of OM, OM/OC, BC, CO, wind speed, temperature, and small-vehicle volume during the study. Large-vehicle volume (not shown) peaked in the midday and was low overnight. Concentrations of OM were highest in the evening hours when wind speeds were low, a ground-level temperature inversion occurred, and a combination of local primary emissions (including residential biomass burning) occurred (Brown et al., 2012). A secondary OM peak typically occurred during the morning rush hour. Traffic volume peaked in the morning and evening hours, with average speed of 67 mph (108 kph). For comparison, BC and CO showed similar concentration peaks in the morning and in the evening.

As further seen in Figure 7, the AMS-derived OM/OC ratio was, on average, higher in the midday (OM/OC = 1.67) and overnight (OM/OC = 1.70 at 0300 LST) than in the morning (OM/OC = 1.55 at 0600 LST) and evening (OM/OC = 1.47 at 2100 LST). The low ratio in the morning hours corresponded with the morning rush hour and typically low wind speeds. Under these conditions and time of day, the predominant source of organic aerosol is likely fresh emissions from the freeway and the larger urban area, with a low amount of SOA. The OM/OC ratio of 1.54 is indicative of fresh aerosol, and in particular of fresh vehicle emissions (Chirico et al., 2010; Reff et al., 2009). The increasing OM/OC ratio during the day is consistent with aerosol aging and SOA production.

Between 1500 LST and 1700 LST, the OM/OC ratio rapidly drops from 1.67 to 1.50, then remains low until the minimum of
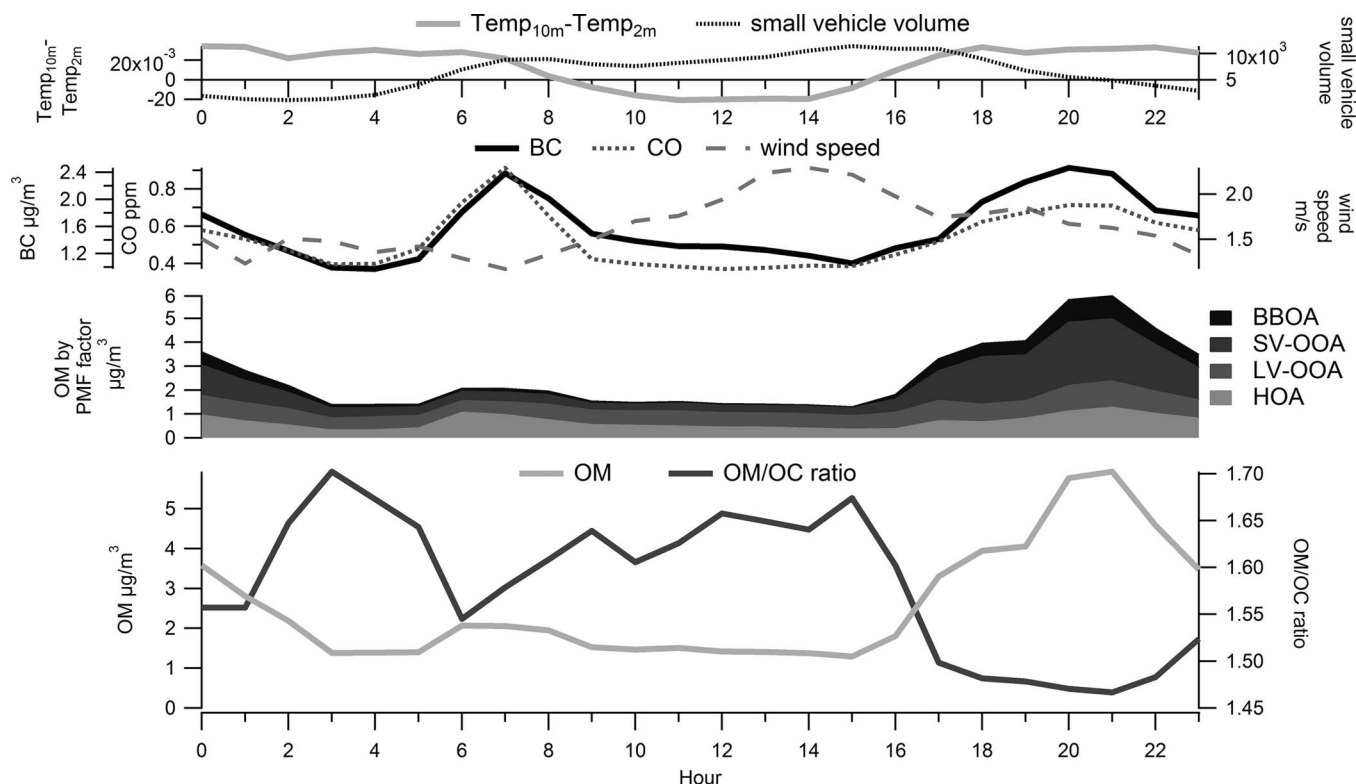


**Figure 4.** Average daily OM/OC ratio, OM concentration ($\mu g/m^3$), temperature (°C), and scalar averaged wind speed (m/sec).

**Figure 6.** Average diurnal pattern of small-vehicle volume (counts/hour × 1000), difference in 10-m and 2-m temperature (positive values indicate a stronger ground-level temperature inversion), BC (μg/m³), CO (ppm), wind speed (m/sec), average concentration by hour and PMF factor (μg/m³), OM (μg/m³), and OM/OC ratio at Fyfe during January 5–28, 2008, by hour (LST).
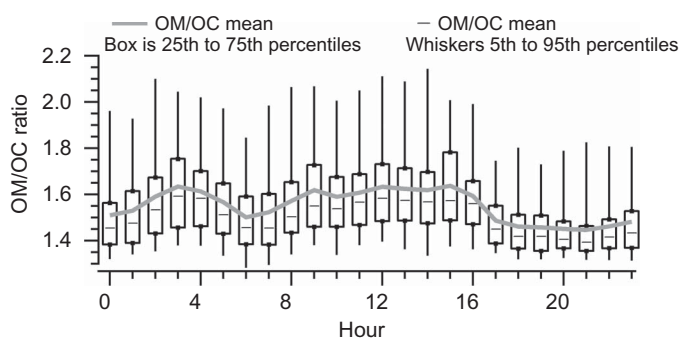


**Figure 7.** Box plot of OM/OC ratio by hour. Mean values are plotted as a continuous line, and medians as dashes inside each box; boxes represent the interquartile range, and whiskers represent the data range to the 5th and 95th percentiles.

1.47 at 2100 LST. During this time, average OM goes from a minimum of 1.3 μg/m³ at 1500 LST to 3.3 μg/m³ at 1700 LST, reaching a peak of 5.9 μg/m³ at 2100 LST, as a combination of vehicular emissions from the evening rush hour and residential biomass burning contributes OM while wind speeds decrease and ground-level temperature inversions occur (Brown et al., 2012).

While examination of diurnal averages is valuable, the aggregation of many data points to calculate the averages may mask additional features in the data. In particular, there are differences in OM/OC ratios both with time of day and with OM concentration. Figure 8 shows the OM/OC ratio versus OM concentration
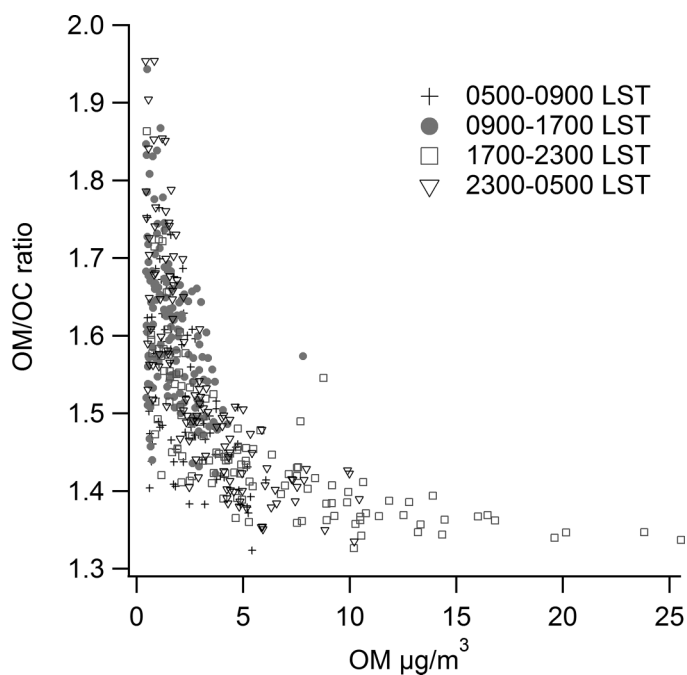


**Figure 8.** OM/OC ratio and OM concentrations (μg/m³) by time of day (LST).

for four times of day: morning rush hour (0500–0900 LST), midday (0900–1700 LST), evening (1700–2300 LST), and overnight (2300–0500 LST). At all times of day, OM/OC is lower and its range is smaller when OM concentrations are higher. The

observed relationship between OM/OC and OM might result from greater gas-to-particle partitioning of more volatile organic compounds when OM is present at higher concentration (Robinson et al., 2007; Lipsky and Robinson, 2006). Cappa and Jimenez (2010) determined that BBOA and primary HOA have the greatest potential for fine particle formation because the semivolatile material associated with BBOA and HOA is most likely to move to the particle phase under high-OM, low-temperature conditions. This semivolatile material has a relatively low OM/OC ratio and can move into the particulate phase under these high OM conditions without first undergoing extensive oxidation. Chan et al. (2010) also demonstrated that OM/OC decreases with increased OM concentrations, though they ascribed this trend to different source mixtures as well as increased partitioning at their site, near Toronto.

The diurnal variations of the Las Vegas OM/OC ratio are largely driven by changes in O/C ratio, and to a lesser degree, H/C ratio. Figures 9 and 10 show the diurnal pattern of O/C and H/C, and Figure 11 shows a scatter plot of H/C versus O/C for hourly averages, also known as a van Krevelen diagram (Heald et al., 2010). H/C is highest in the morning and evening (overall average 1.75), while O/C is highest in the middle of the day (overall average 0.30). On the H/C versus O/C scatter plot, starting in the lower right corner at 0300 LST, average H/C is at its lowest and O/C at its highest. As the morning commute (and associated fresh vehicle emissions) begins, there is a slow increase in H/C and decrease in O/C; at 0600 LST, when the morning commute is nearing its peak, there is a sharp increase in H/C and decrease in O/C. Starting at 0800, H/C slowly decreases
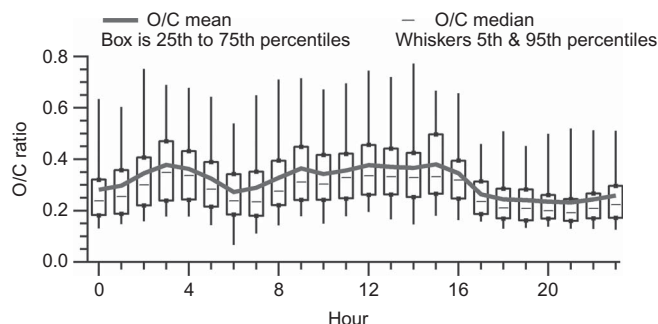


**Figure 11.** Scatter plot of H/C vs. O/C ratio averaged by hour during all hours of January 2008, colored by average OM concentration; each number indicates the hour (LST).

and O/C slowly increases until 1600 LST. During this midday period, mixing heights increase, temperatures rise, and increased atmospheric oxidation occurs, leading to lower OM concentrations and higher O/C. As OM is diluted and temperatures increase, more organic matter can partition to the gas phase; the species partitioning to the gas phase are expected to have lower O/C ratios than the species remaining in the particulate phase, further increasing the O/C ratio of the particulate phase.

By 1700 LST, the evening commute has begun and atmospheric stability increases, leading to a large increase in H/C and a decrease in O/C. Over the next 6 hrs, OM peaks, H/C remains high (evening average of 1.58) and O/C remains relatively low (evening average of 0.24). During the evening, in addition to fresh vehicle emissions, residential biomass burning contributes to OM, as seen via analysis of the data with PMF (Brown et al., 2012). As OM increases and temperature decreases in the evening, more organic compounds can partition to the particulate phase, further increasing OM and the H/C ratio. By 2300 LST, the emissions associated with the evening commute and residential biomass burning have decreased, leading to a slow decrease in OM, a decrease in H/C, and an increase in O/C throughout the night. A number of studies (Donahue et al., 2012; Kroll et al., 2011; Jimenez et al., 2009; Aiken et al., 2008) have demonstrated that direct, primary emissions typically have an O/C of 0–0.17; heavily oxidized organic aerosols have an O/C of 0.67–1; semivolatile organic aerosol has an O/C between 0.33 and 0.67; and biomass burning organic aerosol has a very wide range of 0.07–0.42. Thus, a combination of mobile source and residential biomass burning emissions, in addition to oxidized background organic aerosol, can result in the observed O/C and OM/OC ratios at this Las Vegas site. The reason behind the slow decrease in H/C and corresponding increase in O/C after midnight is unclear; it may reflect a combination of nighttime



**Figure 9.** Box plot of O/C ratios by hour; boxes show the interquartile range, whiskers the 5th and 95th percentiles, dashes the median, and solid line the mean.
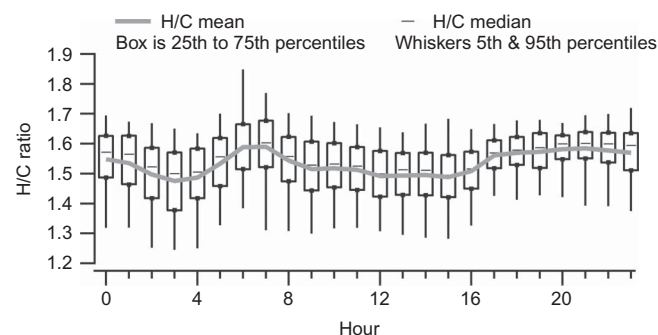


**Figure 10.** Box plot of H/C ratios by hour; boxes show the interquartile range, whiskers the 5th and 95th percentiles, dashes the median, and solid line the mean.
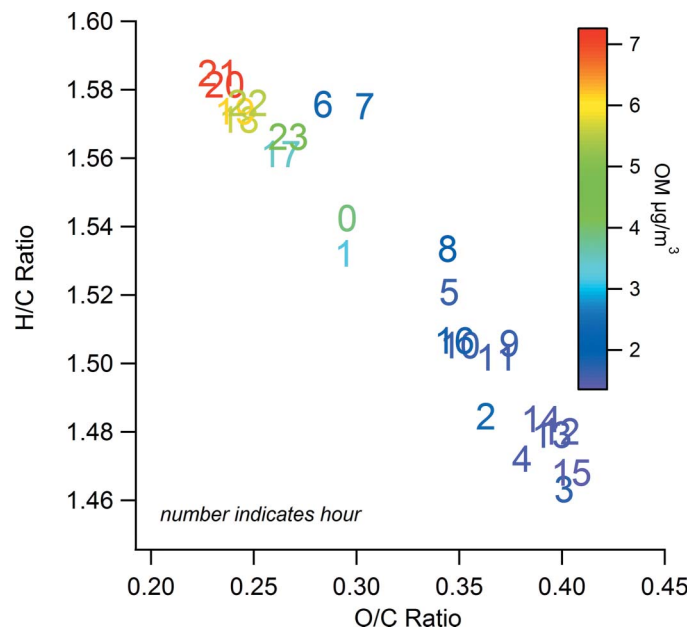
oxidation processes and partitioning to the gas phase of semi-volatile, high-H/C-ratio material, but without coincident gas phase or organic aerosol speciation measurements the exact processes are unknown.

## Variations by wind speed and direction (upwind/downwind)

We also examined how the OM/OC ratio and OM and BC concentrations vary with changes in wind speed and wind direction (i.e., whether the monitoring site is upwind or downwind of the adjacent freeway). OM and BC were higher during low wind periods. Figure 5 shows the relationship of hourly OM with wind speed and OM/OC ratio: Once winds are greater than 2 m/sec, OM is nearly always below 5 $\mu g/m^3$, and the OM/OC ratio is generally greater than 1.6. With low wind speeds, OM is high, and the OM/OC ratio is quite low, averaging 1.4.

BC has a pattern similar to OM, with much higher concentrations when winds are less than 2 m/sec. With higher wind speeds and greater ventilation, aged/oxidized regional aerosol makes up a larger proportion of the OM. Higher wind speeds also cause increased dilution of fresh, low-OM/OC particles, leading to higher OM/OC ratios. Note that lower OM concentrations may lead to the less oxidized material partitioning into the gas phase, reinforcing a higher OM/OC ratio. The opposite is true when higher OM concentrations can lead to more semivolatile, less oxidized material partitioning into the particle phase.

Because concentrations vary significantly by time of day, we compared values during upwind, downwind, and stagnant conditions, grouped into five times of day (Figure 12): overnight (0000–0600), morning (0600–0900), midday (0900–1600), evening (1600–2100), and late evening (2100–0000). During all time periods, OM is consistently higher during stagnant conditions. The OM/OC ratio is broadly similar under all upwind/downwind/stagnant regimes for a given time period. During the morning rush hour, when OM/OC, on average, dips to 1.51, there is no statistical difference in the OM/OC ratio at the 95% confidence level between upwind, downwind, or stagnant conditions. In the midday, wind speeds and ventilation are higher, so concentrations are lower. However, emissions from the freeway

can impact the site quickly if the site is downwind, and since the influence from other fresh emissions is low, the incremental change between downwind and upwind conditions can best be seen at midday. Even though average concentrations are lower at midday, OM is higher and OM/OC lower during downwind conditions compared to upwind conditions at midday. During the 1600–2100 and 2100–0000 LST periods, OM/OC is similar regardless of wind direction, with a median value between 1.41 and 1.45. During the overnight period before the morning rush hour, OM/OC is the most variable, especially during downwind conditions.

## Discussion

The average OM/OC ratio of 1.54 presented here is on the low end of historic ambient measurements but well within the range of 1.3–2.3 found in numerous ambient studies; moreover, it is consistent with the close proximity of the sampling location to a freeway and with reduced wintertime photochemistry. Studies that found values on the higher end of this range took place in locations and/or times of year with more photochemistry and thus higher OM/OC. For example, Mexico City and Riverside summertime average OM/OC ratios were around 1.8 (Williams et al., 2010; Aiken et al., 2008), and the ratio can be even higher at rural sites, such as 2.3 in rural British Columbia (Sun et al., 2009), and 1.9 at rural Midwestern sites (Bae et al., 2006). The average ratio of 1.54 is typical of relatively fresh vehicle or other emissions, such as those generated in laboratory settings (Chirico et al., 2010; Mohr et al., 2009). In Las Vegas during the summertime, the OM/OC ratio would likely be higher, as increased photochemistry would lead to higher oxygen content and higher OM/OC ratios.

The day-to-day variability in the OM/OC ratio is quite large, suggesting that using a fixed OM/OC value, such as the historical default value of 1.4, in PM mass closure calculations, even one that changes seasonally, may be insufficient to achieve accurate mass closure on individual days. In national-scale networks like CSN and IMPROVE, neither OM/OC nor OM is measured; rather, an assumed OM/OC ratio is typically employed to estimate the OM from OC measurements, or the OM/OC ratio may be imputed, for example, by assuming that any $PM_{2.5}$ mass unaccounted for is due to the unmeasured O, H, and N associated with the OC. Since OC often accounts for one-third to one-half of the average $PM_{2.5}$ mass (Hand et al., 2011), the use of a fixed OM/OC ratio is likely the largest uncertainty in trying to achieve mass closure. Simon et al. (2011), examining IMPROVE data, also caution against using a fixed ratio. Even with semicontinuous measurements, such as those from the Sunset OCEC analyzer, OM/OC cannot be determined. Health studies that rely on OC measurements may under- or overestimate exposure to OM, and converting OC to OM with a fixed OM/OC ratio represents a significant source of uncertainty; thus, air quality managers may not have sufficient certainty regarding the importance of OM contributions to $PM_{2.5}$ while making regulatory decisions.

As seen in Figure 8, OM/OC decreases with increasing OM concentrations during this wintertime study. This is especially
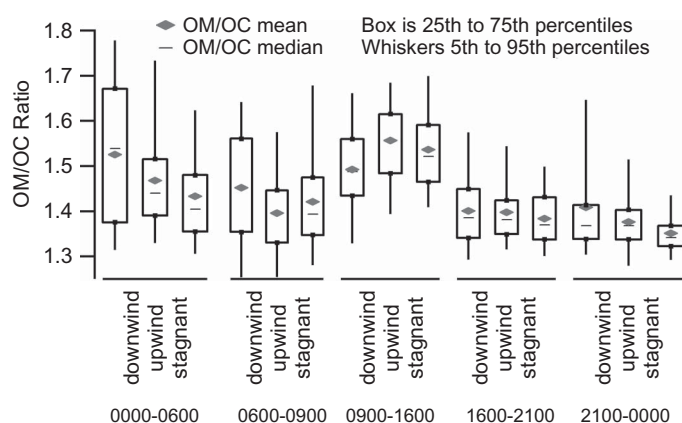


**Figure 12.** OM/OC ratio by time of day bin during downwind, upwind, and stagnant (wind speed < 0.5 m/sec) conditions.

evident in the evening, when mobile source emissions are at a peak, wind speeds are low, and ground-level temperature inversions occur. The low OM/OC with higher OM is likely due to a combination of fresh particulate and semivolatile emissions accompanied by the movement of some semivolatile material into the particle phase as OM concentrations increase. The low OM/OC ratio at high OM concentrations indicates that there may be a large effect from gas-to-particle partitioning of relatively fresh, less oxidized material, because if emissions were first oxidized before partitioning into the particulate phase, the evening OM/OC ratio would likely be higher than the observed 1.4. Robinson (2007) and others have demonstrated that as particulate concentrations increase, semivolatile material is more likely to move into the particle phase. Here, this mechanism may lead to a rapid rise in OM and corresponding decrease in OM/OC ratio in the evening, as fresh, less-oxidized material partitions into the particle phase without first undergoing extensive oxidation.

## Conclusion

The wintertime diurnal and daily variations in OM/OC ratio in Las Vegas were determined using an HR-AMS. HR-AMS measurements correlated well with measurements made by a Sunset OC analyzer. We found that the OM/OC ratio was, on average, 1.54 ($\pm$ 0.20 standard deviation), and the daily average varied between 1.44 and 1.73. OM/OC was generally lowest, approximately 1.4, during the morning and evening hours when OM was highest. A combination of peak emissions and stable atmospheric conditions in the evening may lead to increasing OM and, as more volatile material partitions into the particle phase, decreasing OM/OC. The OM/OC ratio in wintertime Las Vegas is consistent with generally fresh emissions, in contrast to summertime ratios in other cities where the OM is more oxidized and the OM/OC ratio is higher.

## Acknowledgment

## References

Adonis, M.I., R.M. Riquelme, V.D. Martinez, L. Gil, C. Rios, L. Rodriquez, and E.M. Rodriquez. 2003. PAHs and mutagenicity of inhalable and respirable diesel particulate matter in Santiago, Chile. *Polycyclic Aromatic Compounds* 23:495–514. doi:10.1080/714040942

Aiken, A.C., P. DeCarlo, and J.L. Jimenez. 2007. Elemental analysis of organic species with electron ionization high-resolution mass spectrometry. *Anal. Chem. (Washington)* 79:8350–58. doi:10.1021/ac071150w

Aiken, A.C., P. DeCarlo, J.H. Kroll, D.R. Worsnop, J.A. Huffman, K.S. Docherty, I.M. Ulbrich, C. Mohr, J.R. Kimmel, D. Sueper, et al. 2008. O/C and OM/OC ratios of primary, secondary, and ambient organic aerosols with high-resolution time-of-flight aerosol mass spectrometry. *Environ. Sci. Technol.* 42:4478–85. doi:10.1021/es703009q

Aiken, A.C., D. Salcedo, M.J. Cubison, J.A. Huffman, P.F. DeCarlo, I.M. Ulbrich, K.S. Docherty, D. Sueper, J.R. Kimmel, D.R. Worsnop, et al. 2009. Mexico City aerosol analysis during MILAGRO using high resolution aerosol mass spectrometry at the urban supersite (T0). Part 1: Fine particle composition and organic source apportionment. *Atmos. Chem. Phys.* 9:6633–53. doi:10.5194/acp-9-6633-2009

Allan, J.D., A.E. Delia, H. Coe, K.N. Bower, M.R. Alfarra, J.L. Jimenez, A.M. Middlebrook, F. Drewnick, T.B. Onasch, M.R. Canagaratna, et al. 2004. A generalised method for the extraction of chemically resolved mass spectra from Aerodyne aerosol mass spectrometer data. *J. Aerosol Sci.* 35:909–22. doi:10.1016/j.jaerosci.2004.02.007

Bae, M.S., J.J. Schauer, J.T. DeMinter, and J.R. Turner. 2004. Hourly and daily patterns of particle-phase organic and elemental carbon concentrations in the urban atmosphere. *J. Air Waste Manage. Assoc.* 54:823–33. doi:10.1080/10473289.2004.10470957

Bae, M.S., J.J. Schauer, J.T. DeMinter, J.R. Turner, D. Smith, and R.A. Cary. 2004. Validation of a semi-continuous instrument for elemental carbon and organic carbon using a thermal-optical method. *Atmos. Environ.* 38:2885–93. doi:10.1016/j.atmosenv.2004.02.027

Bae, M.S., J.J. Schauer, and J.R. Turner. 2006. Estimation of the monthly average ratios of organic mass to organic carbon for fine particulate matter at an urban site. *Aerosol Sci. Technol.* 40:1123–39. doi:10.1080/02786820601004085

Bauer, J.J., X.-Y. Yu, R. Cary, N. Laulainen, and C. Berkowitz. 2009. Characterization of the sunset semi-continuous carbon aerosol analyzer. *J. Air Waste Manage. Assoc.* 59:826–33. doi:10.3155/1047-3289.59.7.826

Brown, S.G., T. Lee, G.A. Norris, P.T. Roberts, J.L. Collett, Jr., P. Paatero, and D.R. Worsnop. 2012. Receptor modeling of near-roadway aerosol mass spectrometer data in Las Vegas, Nevada, with EPA PMF. *Atmospheric Chemistry and Physics* 12:309–25. doi:10.5194/acp-12-309-2012, STI-3873

Canagaratna, M.R., J.T. Jayne, J.L. Jimenez, J.D. Allan, M.R. Alfarra, Q. Zhang, T.B. Onasch, F. Drewnick, H. Coe, A. Middlebrook, et al. 2007. Chemical and microphysical characterization of ambient aerosols with the Aerodyne aerosol mass spectrometer. *Mass Spectrom. Rev.* 26:185–222. doi:10.1002/mas.20115

Cappa, C.D., and J.L. Jimenez. 2010. Quantitative estimates of the volatility of ambient organic aerosol. *Atmos. Chem. Phys.* 10:5409–24. doi:10.5194/acp-10-5409-2010

Chan, T.W., L. Huang, W.R. Leaitch, S. Sharma, J.R. Brook, J.G. Slowik, J.P.D. Abbatt, P.C. Brickell, J. Liggio, S.-M. Li, and H. Moosmuller. 2010. Observations of OM/OC and specific attenuation coefficients (SAC) in ambient fine PM at a rural site in central Ontario, Canada. *Atmos. Chem. Phys.* 10:2393–411. doi:10.5194/acp-10-2393-2010

Chhabra, P.S., R.C. Flagan, and J.H. Seinfeld. 2010. Elemental analysis of chamber organic aerosol using an aerodyne high-resolution aerosol mass spectrometer. *Atmos. Chem. Phys.* 10: 4111–31. doi:10.5194/acp-10-4111-2010

Chirico, R., P.F. DeCarlo, M.F. Heringa, T. Tritscher, R. Richter, A.S.H. Prévôt, J. Dommen, E. Weingartner, G. Wehrle, M. Gysel, et al. 2010. Impact of after-treatment devices on primary emissions and secondary organic aerosol formation potential from in-use diesel vehicles: results from smog chamber experiments. *Atmos. Chem. Phys.* 10:11545–63. doi:10.5194/acp-10-11545-2010

Chow, J.C., J.G. Watson, D. Crow, D.H. Lowenthal, and T. Merrifield. 2001. Comparison of IMPROVE and NIOSH carbon measurements. *Aerosol Sci. Technol.* 34:23–34. doi:10.1080/02786820119073

de Gouw, J.A., C.A. Brock, E.L. Atlas, T.S. Bates, F.C. Rehsenfeld, P.D. Goldan, J.S. Holloway, W.C. Kuster, B.M. Lerner, B.M. Matthew, A.M. Middlebrook, et al. 2008. Sources of particulate matter in the northeastern United States in summer: Direct emissions and secondary formation of organic matter in urban plumes. *J. Geophys. Res.* 113:1–19. doi:10.1029/2007JD009243

de Gouw, J.A., A.M. Middlebrook, C. Warneke, P.D. Goldan, W.C. Kuster, J.M. Roberts, F.C. Fehsenfeld, D.R. Worsnop, M.R. Canagaratna, A.A.P. Pszenny,

et al. 2005. Budget of organic carbon in a polluted atmosphere: Results from the New England Air Quality Study in 2002. *J. Geophys. Res.* 110:D16305. doi:10.1029/2004JD005623

DeCarlo, P., J.R. Kimmel, A. Trimborn, M. Northway, J.T. Jayne, A.C. Aiken, M. Gonin, K. Fuhrer, T. Horvath, K.S. Docherty, D.R. Worsnop, and J.L. Jimenez. 2006. Field-deployable, high-resolution, time-of-flight aerosol mass spectrometer. *Anal. Chem. (Washington)* 78:8281–89. doi:10.1021/ac061249n

Docherty, K.S., A.C. Aiken, J.A. Huffman, I.M. Ulbrich, P.F. DeCarlo, D. Sueper, D.R. Worsnop, D.C. Snyder, R.E. Peltier, R.J. Weber, B.D. Grover, et al. 2011. The 2005 study of organic aerosols at Riverside (SOAR-1): Instrumental intercomparisons and fine particle composition. *Atmos. Chem. Phys.* 11:12387–420. doi:10.5194/acp-11-12387-2011

Donahue, N.M., J.H. Kroll, S.N. Pandis, and A.L. Robinson. 2012. A two-dimensional volatility basis set—Part 2: Diagnostics of organic-aerosol evolution. *Atmos. Chem. Phys.* 12:615–34. doi:10.5194/acp-12-615-2012

Drewnick, F., S.S. Hings, P. DeCarlo, J.T. Jayne, M. Gonin, K. Fuhrer, S. Weimer, J.L. Jimenez, K.L. Demerjian, S. Borrmann, and D.R. Worsnop. 2005. A new time-of-flight aerosol mass spectrometer (TOF-AMS)—Instrument description and first field deployment. *Aerosol Sci. Technol.* 39:637–58. doi:10.1080/02786820500182040

Edwards, J., S. Walters, and R.K. Griffiths. 1994. Hospital admissions for asthma in preschool children: relationship to major roads in Birmingham, United Kingdom. *Arch. Environ. Health* 49(4): 223–27. doi:10.1080/00039896.1994.9937471

Finkelstein, M.M., M. Jerrett, and M.R. Sears. 2004. Traffic air pollution and mortality rate advancement periods. *Am. J. Epidemiol.* 160(2): 173–77. doi:10.1093/aje/kwh181

Flowers, L., S.H. Rieth, V.J. Cogliano, G.L. Foureman, R. Hertzberg, E.L. Hofmann, D.L. Murphy, S. Nesnow, and R.S. Schoeny. 2002. Health assessment of polycyclic aromatic hydrocarbon mixtures: Current practices and future directions. *Polycyclic Aromatic Compounds* 22:811–21. doi:10.1080/10406630213574

Gilardoni, S., S. Liu, S. Takahama, L.M. Russell, J.D. Allan, R. Steinbrecher, J.L. Jimenez, P.F. DeCarlo, E.J. Dunlea, and D. Baumgardner. 2009. Characterization of organic ambient aerosol during MIRAGE 2006 on three platforms. *Atmos. Chem. Phys.* 9:5417–32. doi:10.5194/acp-9-5417-2009

Hand, J.L., S.A. Copeland, D.E. Day, A.M. Dillner, H. Indresand, W.C. Malm, C.E. McDade, C.T. Moore, M.L. Pitchford, B.A. Schichtel, and J.G. Watson. 2011. Spatial and seasonal patterns and temporal variability of haze and its constituents in the United States: IMPROVE Report V. http://vista.cira.colostate.edu/improve/publications/reports/2011/2011.htm

Heald, C.L., J.H. Kroll, J.L. Jimenez, K.S. Docherty, P.F. DeCarlo, A.C. Aiken, Q. Chen, S.T. Martin, D.K. Farmer, and P. Artaxo. 2010. A simplified description of the evolution of organic aerosol composition in the atmosphere. *Geophys. Res. Lett.* 37:L08803. doi:10.1029/2010GL042737

Health Effects Institute Panel on the Health Effects of Traffic-Related Air Pollution. 2010. Traffic-related air pollution: A critical review of the literature on emissions, exposure, and health effects. http://pubs.healtheffects.org/view.php?id=34

Hiura, T.S., N. Li, R. Kaplan, M. Horwitz, J.C. Seagrave, and A.E. Nel. 2000. The role of a mitochondrial pathway in the induction of apoptosis by chemicals extracted from diesel exhaust particles. *J. Immunol.* 165:2703–11.

Hoek, G., B. Brunekreef, S. Goldbohm, P. Fischer, and P.A. van den Brandt. 2002. Association between mortality and indicators of traffic-related air pollution in the Netherlands: A cohort study. *Lancet* 360:1203–9. doi:10.1016/S0140-6736(02)11280-3

Isaacman, G., K.R. Wilson, A.W.H. Chan, D.R. Worton, J.R. Kimmel, T. Nah, T. Hohaus, M. Gonin, J.H. Kroll, D.R. Worsnop, and A.H. Goldstein. 2012. Improved resolution of hydrocarbon structures and constitutional isomers in complex mixtures using gas chromatography–vacuum ultraviolet-mass spectrometry. *Anal. Chem.* 84:2335–42. doi:10.1021/ac2030464

Jayne, J.T., D.C. Leard, X.F. Zhang, P. Davidovits, K.A. Smith, C.E. Kolb, and D.R. Worsnop. 2000. Development of an aerosol mass spectrometer for size and composition analysis of submicron particles. *Aerosol Sci. Technol.* 33:49–70. doi:10.1080/027868200410840

Jeong, C.H., P.K. Hopke, E. Kim, and D.W. Lee. 2004. The comparison between thermal-optical transmittance elemental carbon and Aethalometer black carbon measured at multiple monitoring sites. *Atmos. Environ.* 38:5193–204. doi:10.1016/j.atmosenv.2004.02.065

Jimenez, J.L., M.R. Canagaratna, N.M. Donahue, A.S.H. Prévôt, Q. Zhang, J.H. Kroll, P.F. DeCarlo, J.D. Allan, H. Coe, N.L. Ng, et al. 2009. Evolution of organic aerosols in the atmosphere. *Science* 326:1525–29. doi:10.1126/science.1180353

Jimenez, J.L., J.T. Jayne, Q. Shi, C.E. Kolb, D.R. Worsnop, I. Yourshaw, J.H. Seinfeld, R.C. Flagan, X.F. Zhang, K.A. Smith, J.W. Morris, and P. Davidovits. 2003. Ambient aerosol sampling using the Aerodyne Aerosol Mass Spectrometer. *J. Geophys. Res. Atmos.* 108:8425. doi:10.1029/2011JD001213, D7.

Kan, H., A.R. Folsom, M. Cushman, K.M. Rose, W.D. Rosamond, D. Duanping Liao, F.W. Lurmann, and S.J. London. 2010. Traffic exposure and incident venous thromboembolism in the Atherosclerosis Risk in Communities (ARIC) study. *J. Thromb. Haemost.* 9:672–678.

Kan, H., G. Heiss, K.M. Rose, E.A. Whitsel, F. Lurmann, and S.J. London. 2008. Prospective analysis of traffic exposure as a risk factor for incident coronary heart disease: The Atherosclerosis Risk in Communities (ARIC) study. *Environ. Health Perspect.* doi:10.1289/ehp.11290

Kim, J.J., S. Smorodinsky, M. Lipsett, B.C. Singer, A.T. Hodgson, and B. Ostro. 2004. Traffic-related air pollution near busy roads: The East Bay Children's Respiratory Health Study. *Am. J. Respir. Crit. Care Med.* 170:520–26. doi:10.1164/rccm.200403-281OC

Kleindienst, T.E., M. Jaoui, M. Lewandowski, J.H. Offenberg, C.W. Lewis, P.V. Bhave, and E.O. Edney. 2007. Estimates of the contributions of biogenic and anthropogenic hydrocarbons to secondary organic aerosol at a southeastern US location. *Atmos. Environ.* 41:8288–300. doi:10.1016/j.atmosenv.2007.06.045

Kroll, J. H., J.D. Smith, D.L. Che, S.H. Kessler, D.R. Worsnop, and K.R. Wilson. 2009. Measurement of fragmentation and functionalization pathways in the heterogeneous oxidation of oxidized organic aerosol. *Phys. Chem. Chem. Phys.* 11:8005–14. doi:10.1039/B905289e

Kroll, J.H., N.M. Donahue, J.L. Jimenez, S.H. Kessler, M.R. Canagaratna, K.R. Wilson, K.E. Altieri, L. R.Mazzoleni, A.S. Wozniak, H. Bluhm, E.R. Mysak, et al. 2011. Carbon oxidation state as a metric for describing the chemistry of atmospheric organic aerosol. *Nat. Chem.* 3:133–39. doi:10.1038/nchem.948

Kunzli, N., R. Kaiser, S. Medina, M. Studnicka, O. Chanel, and P. Filliger. 2000. Public-health impact of outdoor and traffic-related air pollution: A European assessment. *Lancet* 356:795–801. doi:10.1016/S0140-6736(00)02653-2

Larsen, R.K., and J.E. Baker. 2003. Source apportionment of polycyclic aromatic hydrocarbons in the urban atmosphere: A comparison of three methods. *Environ. Sci. Technol.* 37:1873–81. doi:10.1021/es0206184

Lipsky, E.M., and A.L. Robinson. 2006. Effects of dilution on fine particle mass and partitioning of semivolatile organics in diesel exhaust and wood smoke. *Environ. Sci. Technol.* 40:155–62. doi:10.1021/es050319p

Liu P.S.K., Deng R., Smith K.A., Williams L.R., Jayne J.T., Canagaratna M.R., Moore K., Onasch T.B., Worsnop D.R., and Deshler T. (2007) Transmission efficiency of an aerodynamic focusing lens system: Comparison of model calculations and laboratory measurements for the Aerodyne aerosol mass spectrometer. *Aerosol Sci. Technol.* 41:721–33. doi:10.1080/02786820701422278

Lobscheid, A.B., and T.E. McKone. 2004. Constraining uncertainties about the sources and magnitude of polycyclic aromatic hydrocarbon (PAH) levels in ambient air: The state of Minnesota as a case study. *Atmos. Environ.* 38:5501–15. doi:10.1016/j.atmosenv.2004.06.035

Malm, W.C., J.F. Sisler, D. Huffman, R.A. Eldred, and T.A. Cahill. 1994. Spatial and seasonal trends in particulate concentration and optical extinction in the United States. *J. Geophys. Res.* 99:1347–70. doi:10.1029/93JD02916

Matthew, B.M., A.M. Middlebrook, and T.B. Onasch, Collection efficiencies in an Aerodyne aerosol mass spectrometer as a function of particle phase for laboratory generated aerosols. *Aerosol Sci. Technol.*, 2008. 42:884–98. doi:10.1080/02786820802356797

Maria, S.F., L.M. Russell, B.J. Turpin, R.J. Porcja, T.L. Campos, R.J. Weber, and B.J. Huebert. 2003. Source signatures of carbon monoxide and organic functional groups in Asian Pacific Regional Aerosol Characterization Experiment (ACE-Asia) submicron aerosol types. *J. Geophys. Res* 108:8637. doi:10.1029/2003JD003703

Mauderly, J.L. 1994. Toxicological and epidemiological evidence for health risks from inhaled engine emissions. *Environ. Health Perspect.* 102:165–71. doi:10.2307/3431948

Mohr, C., J.A. Huffman, M. Cubison, A.C. Aiken, K.S. Docherty, J.R. Kimmel, I.M. Ulbrich, M. Hannigan, and J.L. Jimenez. 2009. Characterization of primary organic aerosol emissions from meat cooking, trash burning, and motor vehicles with high-resolution aerosol mass spectrometry and comparison with ambient and chamber observations. *Environ. Sci. Technol.* 43:2443–49. doi:10.1021/es8011518

Nitta, H., T. Sato, S. Nakai, K. Maeda, S. Aoki, and M. Ono. 1993. Respiratory health associated with exposure to automobile exhaust. 1. Results of cross-sectional studies in 1979, 1982, and 1983. *Arch. Environ. Health* 48:53–58. doi:10.1080/00039896.1993.9938393

Polidori, A., B.J. Turpin, C.I. Davidson, L.A. Rodenburg, and F. Maimone. 2008. Organic $PM_{2.5}$: Fractionation by polarity, FTIR spectroscopy, and OM/OC ratio for the Pittsburgh aerosol. *Aerosol Sci. Technol.* 42:233–46. doi:10.1080/02786820801958767

Rattigan, O.V., H.D. Felton, M.-S. Bae, J.J. Schwab, and K.L. Demerjian. 2010. Multi-year hourly PM2.5 carbon measurements in New York: Diurnal, day of week and seasonal patterns. *Atmos. Environ.* 44:2043–53. doi:10.1016/j.atmosenv.2010.01.019

Reff A., Bhave P.V., Simon H., Pace T.G., Pouliot G.A., Mobley J.D., and Houyoux M. 2009. Emissions inventory of $PM_{2.5}$ trace elements across the United States. *Environ. Sci. Technol.* 43:5790–96. doi:10.1021/es802930x

Robinson, A.L., N.M. Donahue, M.K. Shrivastava, E.A. Weitkamp, A.M. Sage, A.P. Grieshop, T.E. Lane, J.R. Pierce, and S.N. Pandis. 2007. Rethinking organic aerosols: Semivolatile emissions and photochemical aging. *Science* 315:1259. doi:10.1126/science.1133061

Rogge, W.F., M.A. Mazurek, L.M. Hildemann, G.R. Cass, and B.R.T. Simoneit. 1993. Quantification of urban organic aerosols at a molecular-level— Identification, abundance and seasonal-variation. *Atmos. Environ. Part A Gen. Topics* 27:1309–30. doi:10.1016/0960-1686(93)90257-Y

Russell, L.M. 2003. Aerosol organic-mass-to-organic-carbon ratio measurements. *Environ. Sci. Technol.* 37:2982–87. doi:10.1021/es026123w

Sage, A.M., E.A. Weitkamp, A.L. Robinson, and N.M. Donahue. 2008. Evolving mass spectra of the oxidized component of organic aerosol: Results from aerosol mass spectrometer analyses of aged diesel emissions. *Atmos. Chem. Phys.* 8:1139–52. doi:10.5194/acp-8-1139-2008

Schauer, J.J., M.J. Kleeman, G.R. Cass, and B.R.T. Simoneit. 2002. Measurement of emissions from air pollution sources. 5. C-1-C-32 organic compounds from gasoline-powered motor vehicles. *Environ. Sci. Technol.* 36:1169–80. doi:10.1021/es0108077

Seagrave, J., J.D. McDonald, E. Bedrick, E.S. Edgerton, A.P. Gigliotti, J.J. Jansen, L. Ke, L.P. Naeher, S.K. Seilkop, M. Zheng, and J.L. Mauderly. 2006. Lung toxicity of ambient particulate matter from southeastern U.S. sites with different contributing sources: Relationships between composition and effects. *Environ. Health Perspect.* 114:1387–93. doi:10.1289/ehp.9234

Simon, H., P.V. Bhave, J.L. Swall, N.H. Frank, and W.C. Malm. 2011. Determining the spatial and seasonal variability in OM/OC ratios across the US using multiple regression. *Atmos. Chem. Phys.* 11:2933–49. doi:10.5194/acp-11-2933-2011

Sin, D.W.M., W.H. Fung, Y.Y. Choi, C.H. Lam, and Y.C. Wong. 2004. Measurement of carbonaceous aerosols: Validation of a thermal gravimetric method and its comparison with a thermal optical transmittance method. *Microchem. J.* 77:63–70. doi:10.1016/j.microc.2003.12.001

Sun, Y., Q. Zhang, A.M. MacDonald, K. Hayden, S.M. Li, J. Liggio, P.S.K. Liu, K.G. Anlauf, W.R. Leaitch, A. Steffen, M. Cubison, D.R. Worsnop, A. van Donkelaar, and R.V. Martin. 2009. Size-resolved aerosol chemistry on Whistler Mountain, Canada with a high-resolution aerosol mass spectrometer during INTEX-B. *Atmos. Chem. Phys.* 9:3095–111. doi:10.5194/acp-9-3095-2009

Takegawa, N., Y. Miyazaki, Y. Kondo, Y. Komazaki, T. Miyakawa, J.L. Jimenez, J.T. Jayne, D.R. Worsnop, J.D. Allan, and R.J. Weber. 2005. Characterization of an Aerodyne aerosol mass spectrometer (AMS): Intercomparison with other aerosol instruments. *Aerosol Sci. Technol.* 39:760–70. doi:10.1080/02786820500243404

Tkacik, D.S., A.A. Presto, N.M. Donahue, and A.L. Robinson. 2012. Secondary organic aerosol formation from intermediate-volatility organic compounds: Cyclic, linear, and branched alkanes. *Environ. Sci. Technol.* 46:8773–81. doi:10.1021/es301112c

Turpin, B.J., and H.-J. Lim. 2001. Species contribution to $PM_{2.5}$ mass concentrations: Revisiting common assumptions for estimating organic mass. *Aerosol Sci. Technol.* 35:602–10. doi:10.1080/02786820119445

Volkamer, R., J.L. Jimenez, F.S. Martini, K. Dzepina, Q. Zhang, D. Salcedo, L.T. Molina, D.R. Worsnop, and M.J. Molina. 2006. Secondary organic aerosol formation from anthropogenic air pollution: Rapid and higher than expected. *Geophys. Res. Lett.* 33:L17811. doi:10.1029/2006GL026899

Washington University Air Quality Laboratory. 2006. User guide for the WUAQL AethDataMasher, version 5.0a. http://users.seas.wustl.edu/jrturner/Aethalometer.htm

Weingartner, E., H. Burtscher, and U. Baltensperger. 1997. Hygroscopic properties of carbon and diesel soot particles. *Atmos. Environ.* 31:2311–2327. doi:10.1016/S1352-2310(97)00023-X

White, W.H., and P.T. Roberts. 1977. On the nature and origin of visibility-reducing aerosols in the Los Angeles Air Basin. *Atmos. Environ.* 11:803–12. doi:10.1016/0004-6981(77)90042-7

Williams, B.J., A.H. Goldstein, N.M. Kreisberg, S.V. Hering, D.R. Worsnop, I.M. Ulbrich, K.S. Docherty, and J.L. Jimenez. 2010. Major components of atmospheric organic aerosol in southern California as determined by hourly measurements of source marker compounds. *Atmos. Chem. Phys.* 10:11577–603. doi:10.5194/acp-10-11577-2010

Zhang, Q., M.R. Canagaratna, J.T. Jayne, D.R. Worsnop, and J.-L. Jimenez. 2005. Time- and size-resolved chemical composition of submicron particles in Pittsburgh: Implications for aerosol sources and processes. *J. Geophys. Res.* 1(10):D07S09. doi:10.1029/2004JD004649

## About the Authors

**Steven G. Brown** is Manager of the Aerometric Data Analysis Group, and **Paul T. Roberts** is Executive Vice President at Sonoma Technology, Inc., Petaluma, CA.

**Taehyoung Lee** is an assistant professor in the Department of Environmental Science, Hankuk University of Foreign Studies, Yongin, Republic of Korea, and **Jeffrey L. Collett, Jr.,** is Department Head at the Atmospheric Science Department at Colorado State University, Fort Collins, CO.